

RESEARCH PAPER

## Morphological, Structural and Photoresponse Characterization of ZnO Nanostructure Films Deposited on Plasma Etched Silicon Substrates

Bassam Abdallah\*, Abdul Kader Jazmati, Feras Nounou

Atomic Energy Commission, Department of Physics, P. O. Box 6091, Damascus, Syria

### ARTICLE INFO

#### Article History:

Received 12 September 2019

Accepted 05 November 2019

Published 01 January 2020

#### Keywords:

Morphology

Nanostructures

Optical reflectance

Photoresponse

ZnO films

### ABSTRACT

ZnO nanostructure films were deposited by radio frequency (RF) magnetron sputtering on etched silicon (100) substrates etched using dry Ar/SF<sub>6</sub> plasma, at two etching times of 5 min and 30 min, and on non etched silicon surface. Energy dispersive X-ray (EDX) technique was employed to investigate the elements contents for etched substrates as well as ZnO films, where it is found to be stoichiometric. Surface and growth evolution of films were explored by scanning electron microscope (SEM) images and found to have morphological development from spherical forms into nanowires with increasing substrate etching time. 2D atomic force microscope (AFM) images clarify this modification of the morphology and roughness values are deduced. Structural study was investigated using X-ray diffraction (XRD) patterns. The films had (002) preferential orientation with various etching time substrates. Optical characterization illustrated a decrease of reflectance with the morphological modification. Photoresponse measurement has been investigated and correlated with the crystallinity.

### How to cite this article

Abdallah B, Jazmati AK, Nounou F. Morphological, Structural and Photoresponse Characterization of ZnO Nanostructure Films Deposited on Plasma Etched Silicon Substrates. J Nanostruct, 2020; 10(1): 185-197. DOI: 10.22052/JNS.2020.01.020

### INTRODUCTION

The surface morphology, size, form and nanostructure affect the physical, chemical and electrical properties of thin films relative to the bulk behavior especially in semiconducting materials [1]. Recently a controlled ZnO nanostructure plays a crucial role in optoelectronic devices performance. In general, one can manipulate and adjust the nanostructure [2] to form nanosphere, core-shell, nanorod and nanowire by two ways. Firstly by variation of the synthesis parameter such as power, pressure and oxygen percentage [3] in techniques using plasma like magnetron sputtering [4], secondly, by the pre-treatment of the substrate surface [5], such as by chemical etching [6] or dry etching in plasma [7, 8].

\* Corresponding Author Email: [pscientific27@aec.org.sy](mailto:pscientific27@aec.org.sy)

There was a great interest from researchers of the properties of Si/ZnO heterojunction devices [9-11], where a planar silicon substrate was used [12-14]. However, recently, researchers began to be interested to study Si/ZnO heterojunctions based on Si-nanostructures [15-17].

The crystallographic structure such as orientation, grain size and growth mechanism play a potential role in the films properties including physical [18] [19], mechanical, electrical, optical [20] and sensing [19, 1] behaviors especially in the case of proffered preferred orientation existence.

The sensitivity response of WO<sub>3</sub>, ZnO or SnO<sub>2</sub> doped Zn depends on many parameters where the most important ones are the temperature and the surface morphology [1, 21, 22].

Bruno et al [1] have studied the response of ZnO nanowalls for CO and NO<sub>2</sub> gases. In our recent study concerning sensitivity at room temperature for WO<sub>3</sub> [23] and SnO<sub>2</sub> films, where the sensitivity is investigated and related to crystallographer orientation [23]. The differences in the optoelectronic properties in the ZnO nanostructures are due to the quantum confinement effect originated from nanoscale dimensions [22].

Different processes have been applied to prepare semiconductor films for example ZnO, SnO<sub>2</sub> [19], and ZnS [24] nanostructures of different morphologies including sol gel [2, 25] ultrasonic spray pyrolysis [19] thermal evaporation, metal-organic chemical vapor deposition (MOCVD), molecular beam epitaxy (MBE) and physical vapor deposition (PVD) including pulsed laser deposition [26] and magnetron sputtering. In the later method, high quality films can be produced with a controlled thickness [27] and orientation. The good adhesion between substrate and films can be obtained by using DC or RF magnetron sputtering at room temperature [3,20] while other techniques require high temperature which, in turn, can limit the substrate types like polymers and glass [28, 29].

M. Naddaf, et al [6] have investigated the effect of surface pre-treatments by anodic etching electrolyte on GaAs substrates, on structural and optical properties of Al doped zinc oxide (AZO) thin films. Rusli et al [30] have studied the effect of porosity with a pore diameter of 15 to 40 nm on ZnO nanorods films properties. One of the methods used to obtain silicon nanostructures is dry plasma etching on silicon, which may be more compatible with the silicon fabrication technology than wet etching, plasma excited in SF<sub>6</sub> and its mixture with several gases is widely used for silicon etching [7, 31- 33].

In this work, ZnO thin films, prepared by RF magnetron sputtering, were deposited on planar (polished) Si as well as on Si-nanostructures prepared in Ar/SF<sub>6</sub> plasma dry etching system, where up to our knowledge this is the first time that silicon substrate has been treated by dry plasma in the purpose of obtaining nanostructure ZnO thin films. The morphological characterization was studied using SEM and AFM techniques and the structural properties of deposited thin films were investigated by XRD.

## MATERIALS AND METHODS

PLASSYS-MP600S (French) system has been used to prepare ZnO/Si(100) starting from ZnO target. The details of the synthesized conditions are reported in our recent study [5]. Stoe transmission X-ray diffractometer Stadi P (Cu K $\alpha$ ,  $\lambda = 0.15405$  nm with configuration  $\theta-2\theta$ ) has been used to investigate the structural characterizations of the deposited films. 300 W power of RF (13.56MHz) generator for Plasma Enhanced Chemical Vapor Deposition (PECVD), has been employed to etch silicon substrates with two times (5 and 30 min) where the mixing gas in the chamber is 5% Ar/SF<sub>6</sub> with work pressure of 30 Pa [7]. Details of the used experimental set-up of RF remote plasma system for silicon surface etching was described elsewhere [12, 13]. TSCAN Vega II XMU (Czech Republic) Scanning Electron Microscope (SEM) and Park Scientific Instruments AP-0100 Atomic Force Microscope (AFM) have been utilized to characterize the morphological properties of the ZnO films and substrates. Root Mean Square roughness (RMS), particle density ( $\mu\text{m}^{-2}$ ), mean pore and particle sizes, maximum height ( $R_z$ ) and porosity have been deduced via Gwyddion software. Energy Dispersive X-ray (EDX) spectroscopy has been used to explore the element composition of the films.

## RESULTS AND DISCUSSION

### SEM study

#### Surface study

Fig. 1a and Fig. 1b showed the SEM images of surface silicon substrate etched for 5 min with 20k and 40k magnifications respectively. Similarly, Fig. 1c and Fig. 1d showed the SEM images for 30 min etching with 20k and 40k magnifications as well.

SEM, generally, can reveal information about surface modifications where for 5 min plasma treatment, silicon substrate starts to form small pits (pores) as shown in Fig. 1a and Fig. 1b and as the treatment time increased, large pits (cavities) created with about 1-2 micrometer dimensions as shown in Fig. 1c and (d). So plasma treatment influences the surface morphology and roughness [33]. More details about roughness and porosity will be discussed later.

Rusli et al [30] have grown ZnO nanorods on Porous Silicon (PS) prepared by electrochemical etching using thermal evaporation methods with pore diameter ranging from 15 to 40 nm. However,

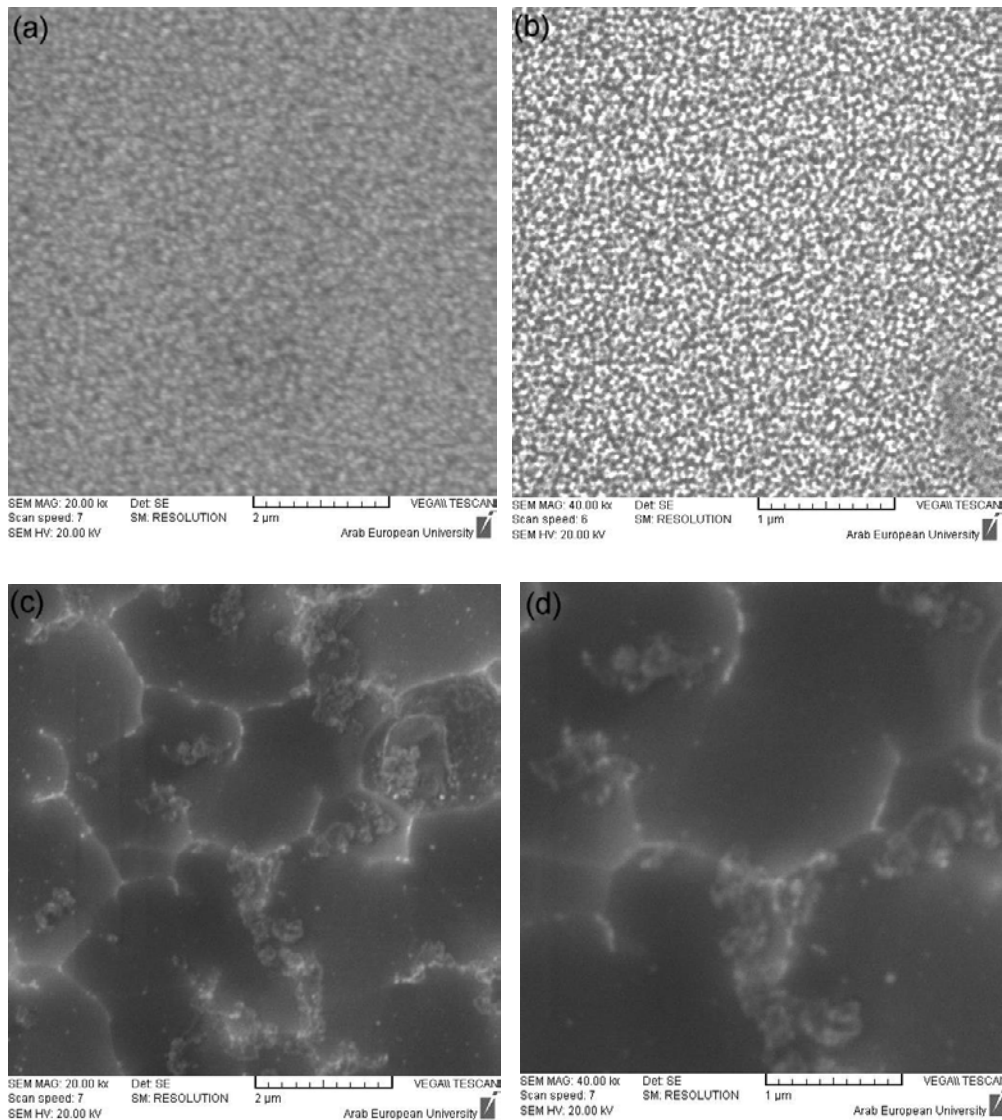


Fig. 1. SEM images of surface Si (100) substrate:(a) and (b) for 5min etching time at 20k and 40k magnification respectively. (c) and (d) for 30min etching time at 20k and 40k magnification respectively.

the films showed polycrystalline structure with hexagonal phase, and it becomes preferred orientation (002) at 800° C temperature. They noted that the morphology of obtained nanorods is affected by etched silicon during initial growth. In our case the porosity of plasma treated Si(100) is less 10 nm for 5 min etching time as shown in (Fig. 1a and Fig. 1b), and it becomes about 1000 nm for 30 min etching time as shown in (Fig. 1c and Fig. 1d). The increasement of the roughness is caused by increasing etching time.

The higher values of the obtained porosity could be due to the type of etching process,

where it was performed in 5% Ar-SF<sub>6</sub> plasma [7]. Choi et al [34] found that the etching rate differs for the two orientations (100) and (111) of the silicon substrates, where Si (100) is higher than Si (111).

Fig. 2a showed surface SEM image of ZnO films deposited on planar substrate (0 min etch). Fig. 2b showed SEM image of films on etched substrate for 5 min. Nano crystalline structures with spherical forms are presented in the Fig. 2a and Fig. 2b and films are still uniform in morphology but the roughness increased for films deposited on etched silicon for 5 min as it is compared with

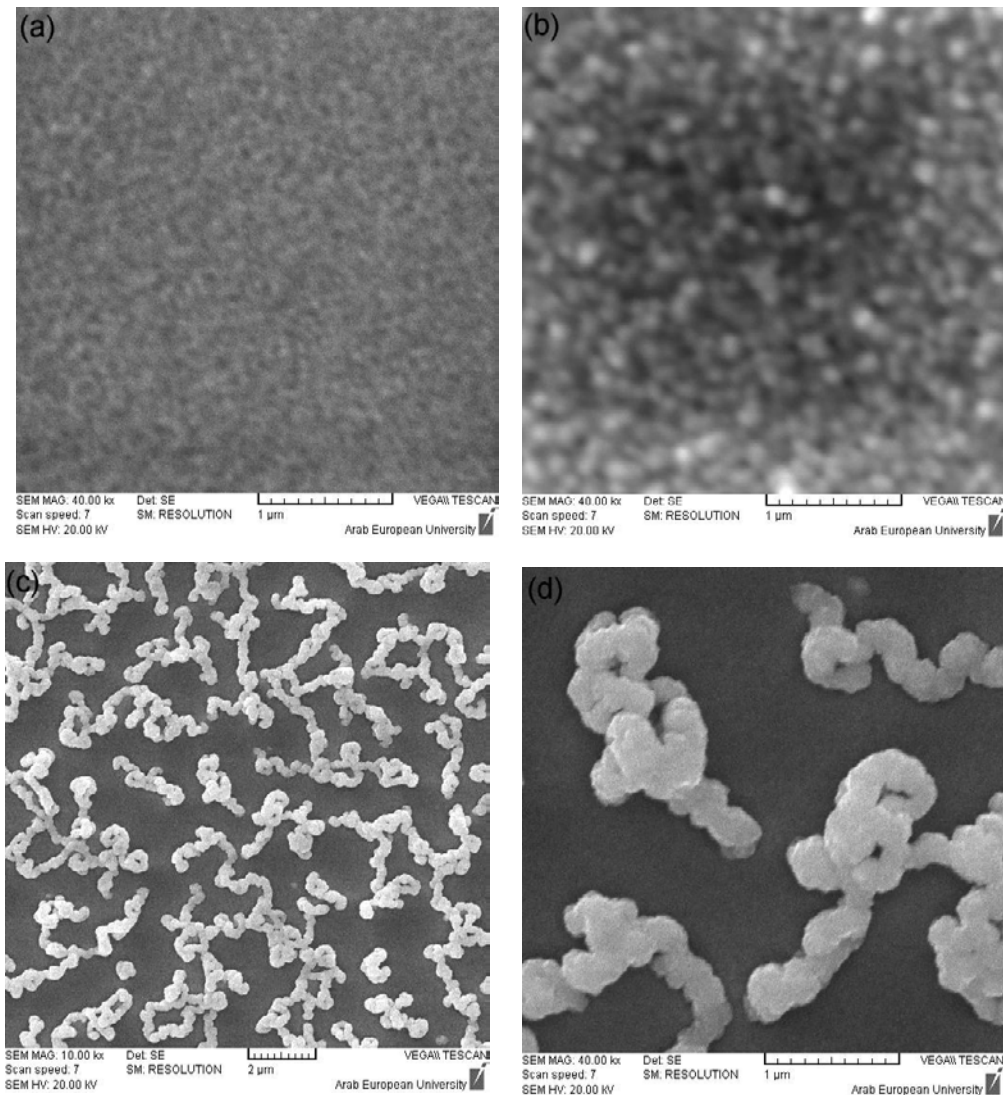


Fig. 2. SEM images of ZnO films: (a) for non etched substrate (MAG: 40K). (b) for 5 min substrate etching time (MAG: 40K). (c) and (d) for 30 min substrate etching time at 10k and 40k magnification respectively.

non etched substrate. This result is consistent with Hazra et al [35] where he demonstrated the core-shell structure of ZnO films deposited on silicon nanowires (NW) heterostructures with SiNWs as core and ZnO thin film as shell prepared by Atomic Layer Deposition.

Fig. 2c and Fig. 2d showed the SEM image for 30 min etching time with 10 and 40 K magnifications, respectively. The films covered the whole surface in the valleys (cavities) and the summits (boundaries). The film on the summits look like string ribbon (wires) and the cross-section images (Fig. 3e and Fig. 3f) will clarify this appearance.

Adding some elements such as Al, Li and Ag

as dopant to ZnO films decreases the etching rate as observed by Shin et al [36]. In addition, the roughness and photoluminescence (PL) of ZnO have been influenced by introducing  $\text{Cl}_2$  in the etching plasma gases as reported by Park et al [37]. Quite the opposite, PL increased for ZnO films prepared via atomic layer deposition (ALD) on Si-nanowires as detected by Chang et al [38].

Rusli et al [30] have studied the ZnO films and found that nanorods have been grown non-uniformly on porous silicon and indicated that there is a difficulty due to lattice mismatch which is important for nucleation of ZnO on Si [39].

Table 1 summarized different techniques that

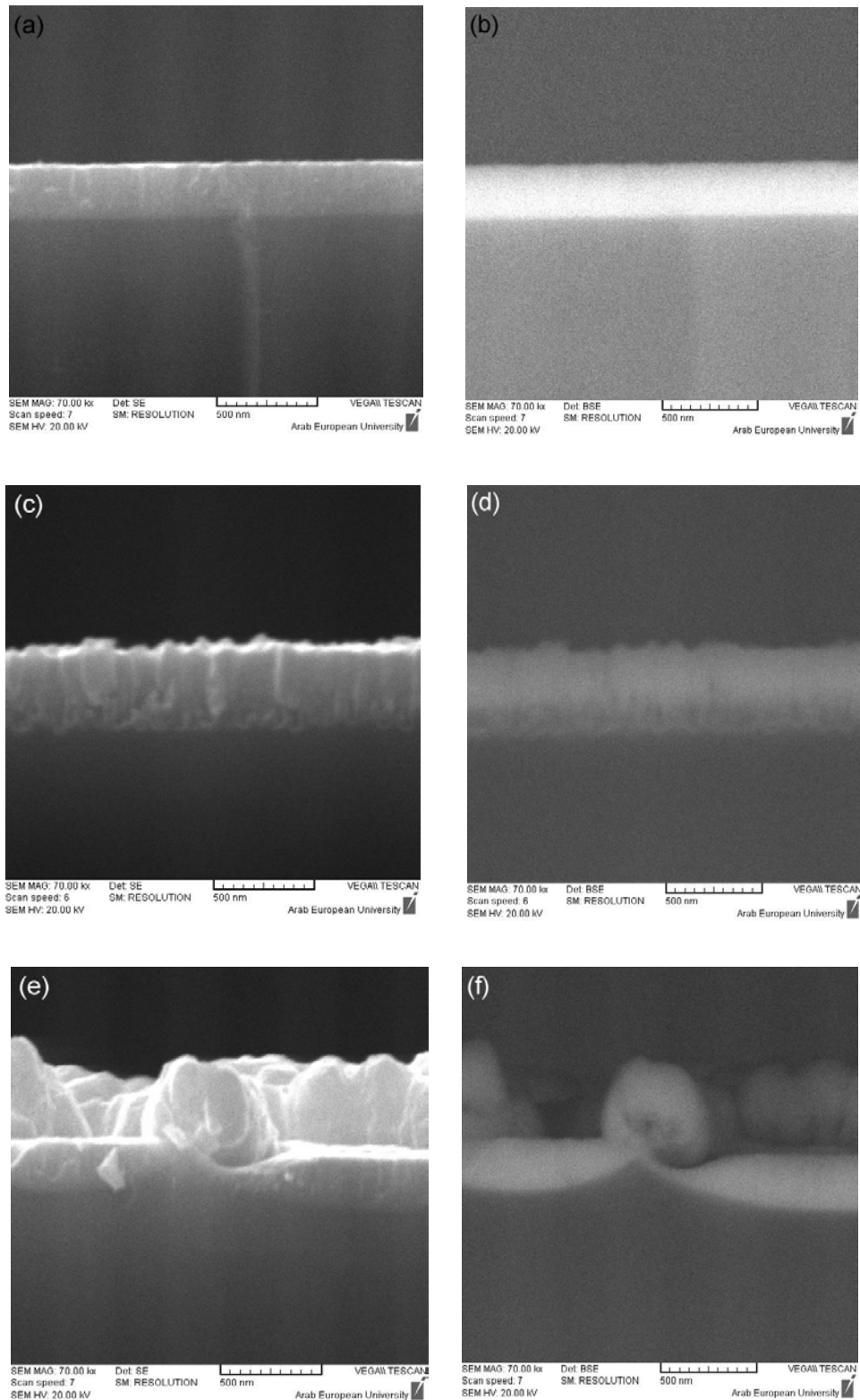


Fig. 3. Cross section SEM images of ZnO/Si films: (a) and (b) for non etched substrate with secondary electron (SE) and Back scattering electron (BSE) detectors respectively. Similarly (c) and (d) for 5 min substrate etching time and (e) and (f) for 30 min substrate etching time.

Table 1. ZnO morphology obtained by different techniques using variant substrate types.

Substrate type	Deposition method	Nanostructure	Reference
Silicon nanowire	Atomic Layer Deposition	core-shell	[35]
porous silicon	Thermal Evaporation	nanorods	[30]
Etched silicon 5 min	Magnetron sputtering	string ribbon	Present work
Etched silicon 30 min		spherical nanostructure	

have been used to synthesize ZnO nanostructure morphology using variant substrate types.

#### Cross section study

Fig. 3a and Fig. 3b are SEM cross-section images, using secondary electron (SE) and backscattering electron (BSE) detectors respectively, for ZnO film deposited on non etched Si (0 min). The measured thickness of the films was about 300nm and it appears to be a dense column growth.

Fig. 3c and Fig. 3d are SEM images for ZnO film deposited on Si etched for 5min using SE and BSE detectors respectively. The film became less dense and thicker and its thickness was about 400 nm with digs in silicon of about 100 nm (pits) due to etching process corresponding to higher roughness.

Fig. 3e and Fig. 3f are images for ZnO film deposited on Si etched for 30 min using SE and BSE detectors respectively. With more etching time, digs became bigger (cavities or valleys) with depth about 250 nm. The ZnO films on the summits (boundaries) appear as ribbon (wires). Comparable with this result Han-Don Um et al [40] have found that ZnO thickness increased near the bottom of the silicon nanowire because of the overlaying shells of ZnO and subsequently transmittance degradation in the visible region.

#### AFM study

Fig. 4a presents 2D AFM image with ( $5 \times 5 \mu\text{m}^2$ ) dimension and Fig. 4b shows its typical texture line for 5 min etched silicon substrate. Similarly, Fig. 4c presents 2D AFM image with ( $5 \times 5 \mu\text{m}^2$ ) dimension and Fig. 4d shows its typical texture line for 30 min etched silicon substrate.

The images revealed formation of pores (small pits), whose depths were about 30 nm for 5 min etching time (Fig. 4a) and 150 nm for 30 min (Fig. 4c). The substrate silicon surfaces had become rougher due to the chemical attack of fluorine atoms, where RMS (Root mean square) roughness were obtained from AFM measurements and varied from 19 nm to 92 nm with increasing

of etching time. So a significant change in morphology with etching time had been observed, where small pores ranging from 90 nm to 1000 nm with a porosity of 14 % corresponds to 5 min etching time as shown in Fig. 4a and Fig. 4b and cavities (large pore) varied from 150 nm to 1500 nm with a porosity of 30 % corresponds to 30 min etching time as shown in Fig. 4c and Fig. 4d. Table 2 depicts the analytical parameters mentioned above for two silicon substrate etching time.

In order to investigate the effect of the silicon surface morphology on film growth, ZnO films were compared between planar (0 etching time) substrate with 5 min and 30 min etching time of silicon substrate surface.

Fig. 5a shows 2D AFM image with ( $5 \times 5 \mu\text{m}^2$ ) dimension and Fig. 5b presents the typical texture line for ZnO film deposited on zero etching time substrate surface. It explains the existence of nanostructure in spherical forms with a diameter of about 73 nm and low roughness (RMS) about 5 nm.

Fig. 6a and Fig. 6b present 2D AFM images along with their typical texture lines for ZnO films deposited on etched silicon substrate for 5 min. Similarly, Fig. 6c and Fig. 6d present 2D AFM images along with their typical texture lines for ZnO films deposited on etched silicon substrate for 30 min

Fig. 6a and Fig. 2b presented the AFM and SEM images for the same film (5 min etching time), where both figures approve each other and show similar morphology with relatively small spherical nanostructure. Fig. 6c and Fig. 2c presented the AFM and SEM images for the same film (30 min etching time), where both figures approved each other as well and show similar morphology where the film on the summits looks like string ribbon (wires) nanostructure. By comparing between them one can deduce that by increasing the substrate etching time clearly modifies the morphology of the deposited film. We are not aware of people have done similar work (deposited ZnO films on etched silicon dry

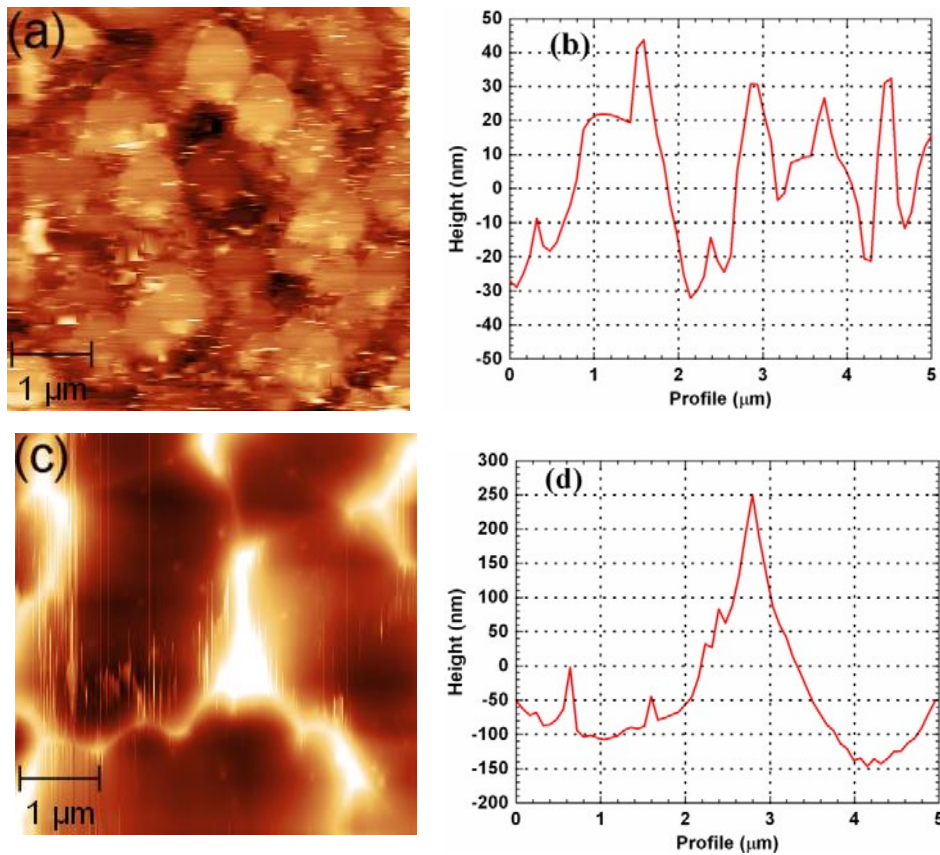


Fig. 4. (a) and (c) 2D AFM image ( $5 \times 5 \mu\text{m}^2$ ) of Si substrate etched for 5 min and 30 min respectively. (b) and (d) typical texture lines of Si substrate etched for 5 min and 30 min respectively.

Table 2. AFM parameters of etched surface silicon in 5%Ar-SF6 plasma for 5 min and 30 min etching times.

Etching time (min)	RMS (nm)	Particle density ( $\mu\text{m}^{-2}$ )	Mean pore size (nm)	Mean particle size (nm)	$R_z$ (nm)	Porosity (%)
5	18	2.2	91	89	180	14
30	92	0.6	445	352	655	30

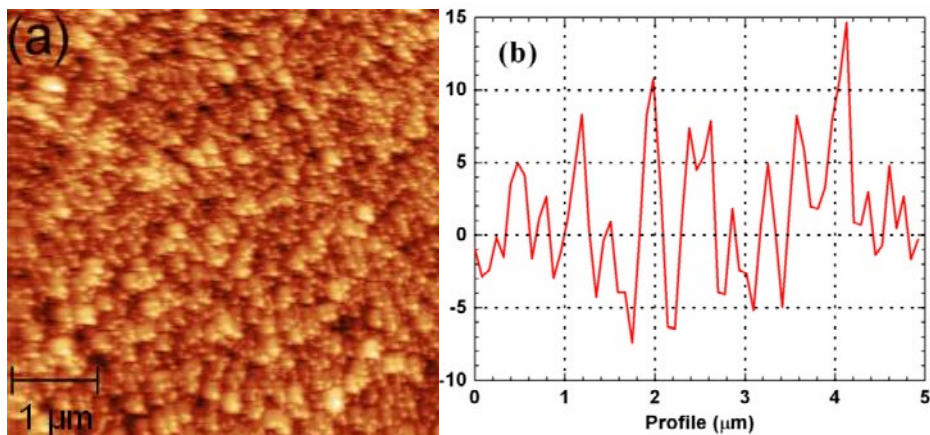


Fig. 5. (a) AFM image and (b) typical texture line of ZnO deposited thin film on zero etching time substrate.

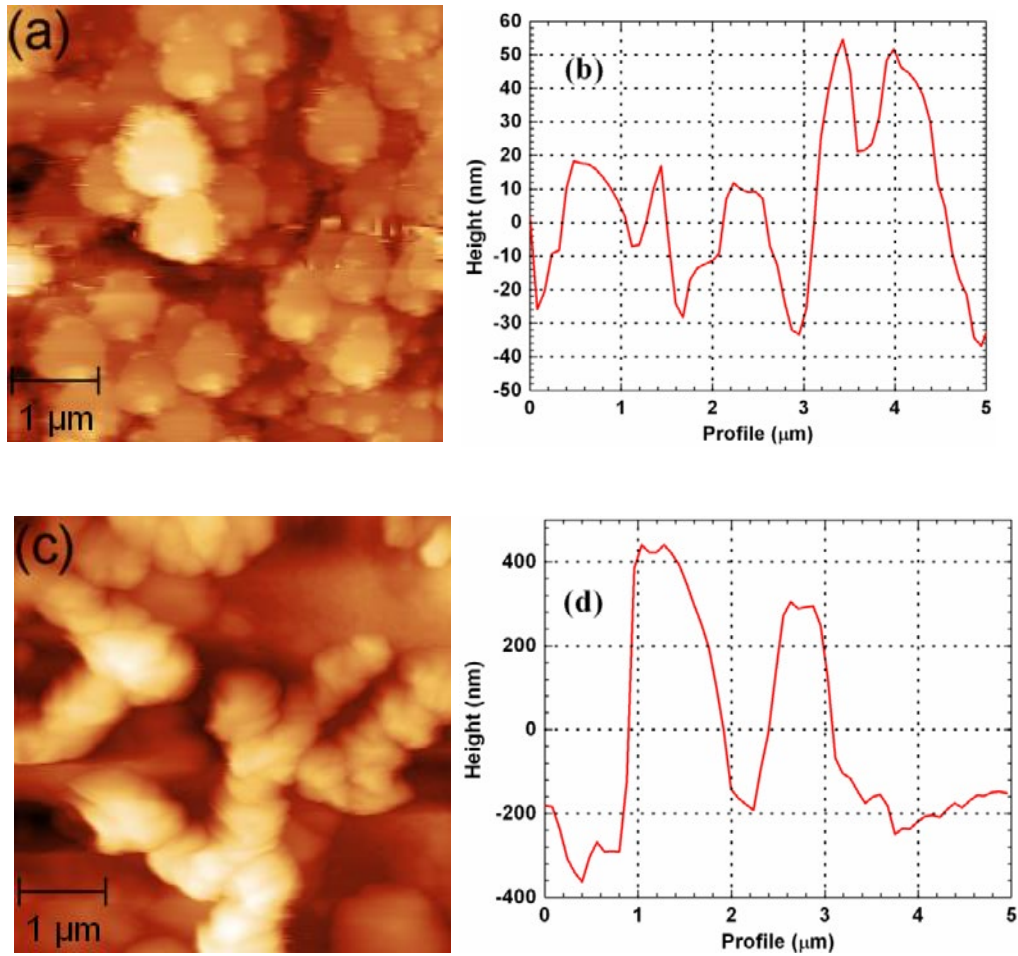


Fig. 6. (a) and (c) 2D AFM images ( $5 \times 5 \mu\text{m}^2$ ) of ZnO films on Si substrate for 5 min and 30 min etching time respectively. (b) and (d) typical texture lines of ZnO films for 5 min and 30 min etching time respectively.

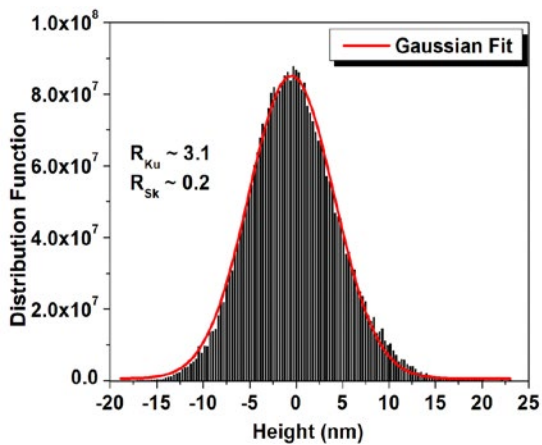


Fig. 7. Histogram of the height distribution function in AFM image of deposited ZnO thin film on zero etching time Si substrate (polished).

$\text{SF}_6$  plasma) to compare with them.

As can be seen from Fig. 5a and Fig. 5b, the ZnO thin film deposited on polished silicon surface exhibits a relatively smooth and dense surface ( $\text{RMS} = 5 \text{ nm}$  and particle density =  $8 \mu\text{m}^{-2}$ ), with a low porosity (1.5%), it had also a relatively uniform particle height distribution as shown in Fig. 7, where the deduced related kurtosis ( $R_{ku}$ : characteristic of surface sharpness) and skewness ( $R_{sk}$ : characteristic of profile symmetry) were found to be equal to 3.1 and 0.2 respectively, which gave a quasi symmetric Gaussian height distribution, it is well known that when the height distribution is Gaussian  $R_{ku} = 3$ , and when it is symmetrical  $R_{sk} = 0$  [41].

Table 3 summarizes the different AFM parameters of deposited ZnO thin film on zero, 5 min and 30 min etching time silicon substrate.



Table 3. AFM parameters of films deposited on etched silicon for zero min, 5 min and 30 min etching times.

Substrate	RMS (nm)	Particle density ( $\mu\text{m}^{-2}$ )	Mean pore size (nm)	Mean particle size (nm)	$R_z$ (nm)	Porosity (%)
Polished Si	5	8.0	41	73	37	1.5
5 min – etched Si	31	2.4	211	280	193	15.0
30 min- etched Si	236	0.5	500	600	1070	28.0

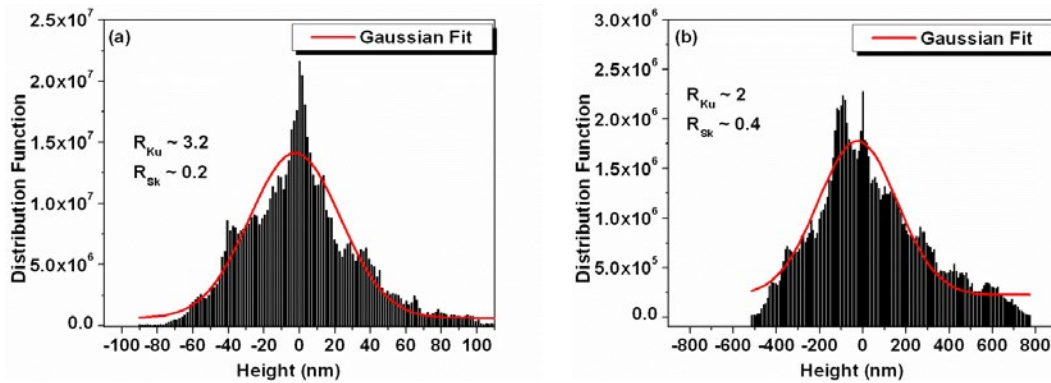


Fig. 8. Histogram of the height distribution function in AFM images of deposited ZnO thin film on etched silicon surface (a) 5 min Si etching time, (b) 30 min Si etching time.

By comparing Fig. 4 and Fig. 6, and Tables 2 and 3, one can see that the morphology of deposited ZnO thin film follows approximately that of substrate (plasma etched Si surface), where the particle density and porosity are rarely changed, while the maximum height, surface roughness and pore and particle sizes are increased due to deposition and incorporation of ZnO particles into the structure of etched silicon surface. Fig. 8a and Fig. 8b presented the plot of the height distribution function of both deposited thin films on 5 min ( $R_{Ku} \sim 3.2$ ,  $R_{Sk} \sim 0.2$ ) and 30 min ( $R_{Ku} \sim 2$ ,  $R_{Sk} \sim 0.4$ ) etched Si substrates respectively. This result indicated that the ZnO thin film is not uniformly deposited on the substrates.

Nayef et al [42] have found the enhancement stability of the structure and studied the surface morphology of ZnO films, using AFM technique, deposited on porous silicon (PS) substrate. However, they found that the film covers almost completely the pores and voids in the sponge-like structure silicon substrate. These ‘pores’ and ‘voids’ play the role in the adhesive surface in the ZnO deposition process.

#### EDX study

Fig. 9 presented the EDX spectrum for the etched silicon substrate (green), where the results

reveal that the main quantity is for silicon in addition to the very low quantity of oxygen (2.16 % At) and fluorine (0.26 % At) elements. For ZnO films deposited on non etched silicon (red line), the ratio O/Zn was found to be about 1 (49.60/50.40 =0.98). Similarly, a close ratio (49.26/50.74=0.97) had been obtained for ZnO film deposited on 5 mints etched silicon (black line). The very small peak at 0.87 KeV corresponded to  $Cu_k$  could be due to contamination from plasma chamber materials.

Abdallah et al [3] showed that ZnO films composition, prepared as a function of oxygen percentage in plasma, were stoichiometric and justified by EDX characterization using the same setup. By increasing oxygen flow the deposition rate decreases and subsequently affects the film crystallinity.

#### Optical reflection study

Optical reflectance property of ZnO thin films was affected by surface morphology and can be correlated to it, this correlation was demonstrated in Fig. 10, which shows the reflectance spectra (R), ranging from 350 nm to 1150 nm of deposited ZnO thin film on (a) zero min, (b) 5 min and (c) 30 min etching time silicon substrate. The inset showed the average reflectance dependence on roughness of deposited thin film surface.

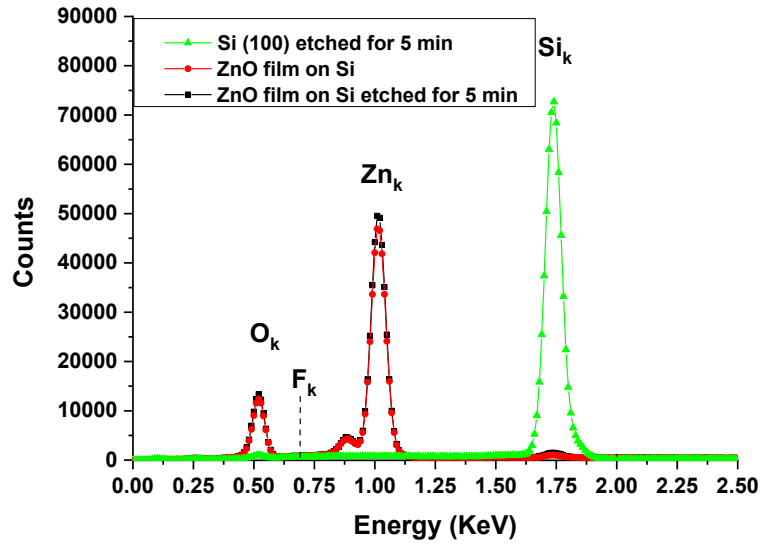


Fig. 9. EDX spectra for silicon substrate etched for 5 mints (green line), ZnO films deposited on the non etched silicon (red line) and 5 mints etched silicon (black line) substrates.

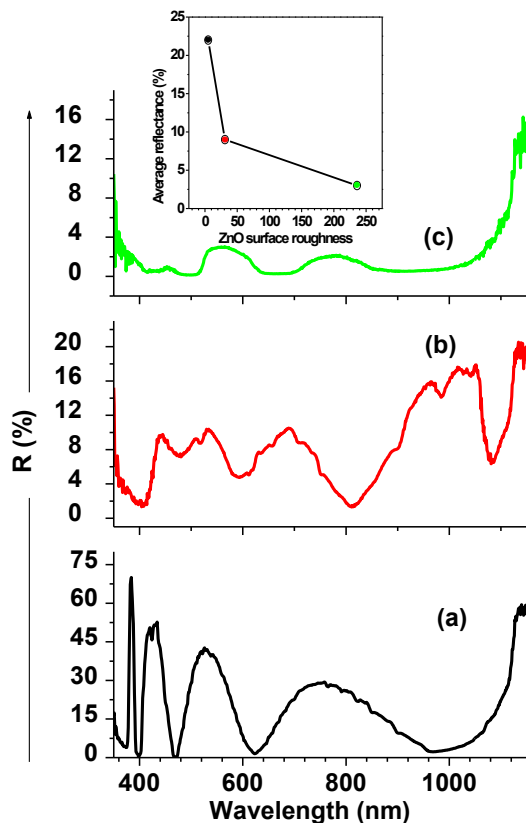


Fig. 10. Reflectance spectra of deposited ZnO thin film on (a) zero min, (b) 5 min and (c) 30 min etching time silicon substrate. The inset shows the evolution of average reflectance as a function of thin film roughness.

It can be seen that Reflectance (R) exhibits interference patterns at various wavelengths. Such a result was previously reported by Cao et al [14], who stated that “Continuously oscillating maxima and minima at different wavelengths suggest the optical homogeneity of deposited thin films”, the continuous oscillation is more evident for deposited thin film on polished silicon rather than on etched Si surface, which is consistent with AFM morphology analysis (Fig. 7 and Fig. 8), where the deposited ZnO thin film on polished silicon (Fig. 7) is more uniform than on etched silicon (Fig. 8). The average reflectance was found to decrease with surface roughness increase due to the effect of light trapping and harvesting by the more roughened structure of deposited ZnO thin films on etched silicon surface.

#### XRD study

ZnO/Si(100) films prepared on different time etched substrates have been characterized by XRD technique. As it is shown in Fig. 11 all the films had preferred orientation (002) corresponding to hexagonal wurtzite structure at about 34.42°, but the intensity of this peak decreased with increasing etching time. However, at for etched silicon substrates (5 min and 30 min etching time), two small peaks appear at 31.4° and 36.25° corresponding to (100) and (101) orientations respectively. The grain size did not develop clear

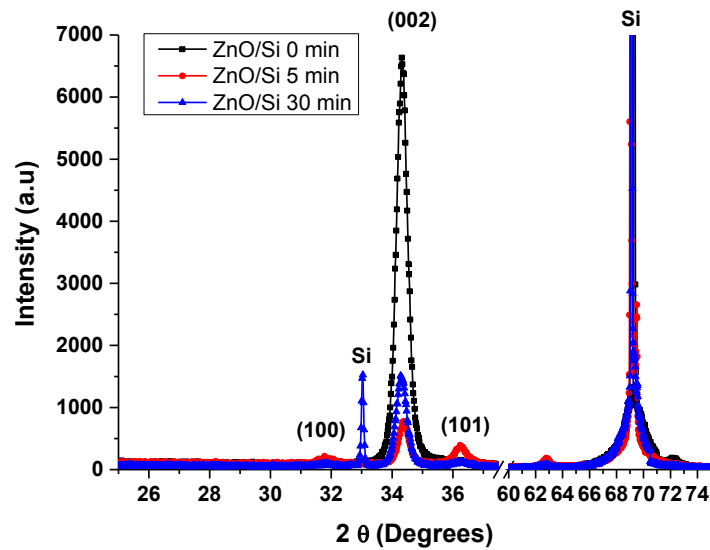


Fig. 11. XRD patterns for ZnO films deposited on Si (100) at 0min, 5min and 30min Etching time substrate.

changes for (002) orientation as it was calculated from Scherrer formula and found to be reduced from 24 nm to 20 nm with increasing etching time. Chebil *et al* [2] have deposited ZnO films on different substrates Si(100), Si(111), glass and Sapphire by sol gel techniques and found no change in the grain size values for (002) peak and attributed that to the lowest surface energy density of the (002) plane.

The non change in the grain size values could be explained by low stress value (less than 1 GPa at such a thickness' range) as it has been measured in previous work for ZnO deposited films [27].

Hazra *et al* [16] have deposited ZnO films on two type of substrate (planar and nano wire silicon) by atomic layer deposition (ALD). Their XRD patterns showed that the films were polycrystalline structure, where (002) and (101) preferred orientation have obtained in film growth on silicon nano wire (SiNW) and non etched silicon (planar) substrate, respectively.

Rusli *et al* [30] have studied depositing of ZnO films on electrochemically etched silicon (100) to become porous (PS) and obtained ZnO nanorods with (002) orientation. They explain that by etching the Si (100), the (111) planes become preferable sites for ZnOx or Zn species to be deposited with good crystalline quality.

The texture factor TC is calculated from the ratio of the XRD peak intensity of (002) orientation relative to the average of the three orientations

[19]. The texture factor of (002) peak of ZnO film was about 0.98, 0.66 and 0.89 for 0, 5 and 30 min etching time for substrate.

#### Photoresponse study

Optoelectronic response was obtained using UV-Vis halogen lamp (jobin-Yvon, France with DC power supply AL924 A) where the density of output optical power was about 0.045 W/m<sup>2</sup> measured by UVA detector. Fig. 12 shows photoresponse for ZnO films deposited on 0, 5 and 30 Si etching time substrate. Where the photocurrent (response), at 1 V bias, rises when UV-Vis halogen lamp switches on/off with interval of about 13 sec. The response and recovery time of the studied films are generally fast about equal to 3 sec. such a fast response and recovery time implies that it is suitable for fast speed operation due to good UV sensing properties. However the photocurrent (response) intensities are 0.003, 0.001 and 0.0005 A for 0, 5 and 30 min etching substrate time respectively. The best response is for ZnO film deposited on non etched substrate, where the texture factor ( $TC_{(002)}=0.98$ ) is maximum and the roughness is lowest value with nanocrystalline structures (spherical forms).

In general, the intensity of the photoresponse corresponds with texture factor behavior mentioned above. This result comes in agreement with Inamdar *et al* [43] where he studied the effect of annealing temperature for ZnO films on the crystallography and photoresponse properties.

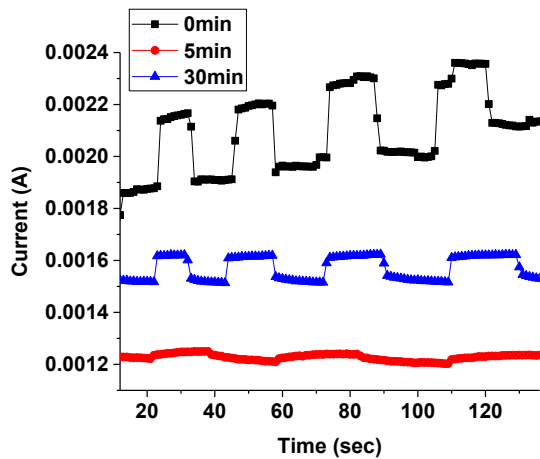


Fig. 12. photoresponse for ZnO films deposited on 0, 5 and 30 Si etching time substrate

## CONCLUSION

The modified morphology of the substrate affected the growth mechanism and developed a nanostructure ZnO films deposited by RF magnetron sputtering. The surface morphology had been changed from spherical particles into nanowires (ribbon) with increasing Ar/SF<sub>6</sub> plasma etching time of the substrate from 0 min to 30 min. The porosity and roughness have been calculated from AFM images and found to be increased with etching time increase. Although morphological development has been observed in the deposited films, no remarkable changes had been detected in the structural properties, where (002) preferred orientation is dominant. The optical reflectance measurements showed a decrease with etching time due to increasing of roughness and observed structural modification. This study indicates a potential application for UV photoresponse of ZnO films.

## ACKNOWLEDGEMENTS

The authors greatly acknowledge funds to this project by Professor I. Othman, the Director General of the Atomic Energy Commission of Syria, Dr. S. Saloum for his valuable discussions and Dr. W. khouri for XRD measurement.

## CONFLICT OF INTEREST

The authors declare that there is no conflict of interests regarding the publication of this manuscript.

## REFERENCE

- Bruno E, Strano V, Mirabella S, Donato N, Leonardi S, Neri G. Comparison of the Sensing Properties of ZnO Nanowalls-Based Sensors toward Low Concentrations of CO and NO<sub>2</sub>. *Chemosensors*. 2017;5(3):20.
- Chebil W, Fourozi A, Azeza B, Sakly N, Mghaieth R, Lusson A, et al. Comparison of ZnO thin films on different substrates obtained by sol-gel process and deposited by spin-coating technique *Indian J Pure Appl Phys*. 2015;53:521-529.
- Abdallah B, Jazmati AK, Refaai R. Oxygen Effect on Structural and Optical Properties of ZnO Thin Films Deposited by RF Magnetron Sputtering. *Materials Research*. 2017;20(3):607-12.
- Rahmane S, Djouadi MA, Aida MS, Barreau N, Abdallah B, Hadj Zoubir N. Power and pressure effects upon magnetron sputtered aluminum doped ZnO films properties. *Thin Solid Films*. 2010;519(1):5-10.
- Jazmati AK, Abdallah B, Lahlah F, Abou Shaker S. Photoluminescence and optical response of ZnO films deposited on silicon and glass substrates. *Materials Research Express*. 2019;6(8):086401.
- Naddaf M, Saad M. Comparative study of structural and visible luminescence properties of AZO thin film deposited on GaAs and porous GaAs substrates. *Vacuum*. 2015;122:36-42.
- Saloum S, Akel M, Alkhaled B. Diagnostic and processing in SF<sub>6</sub>RF remote plasma for silicon etching. *Journal of Physics D: Applied Physics*. 2009;42(17):175206.
- Saloum S, Zrir MA, Alkhaled B, Shaker SA. Silicon Nanostructuring Using SF<sub>6</sub>/O<sub>2</sub> Downstream Plasma Etching: Morphological, Optical and Sensing Properties. *Materials Research*. 2018;21(5).
- Jung BO, Lee JH, Lee JY, Kim JH, Cho HK. High-Purity Ultraviolet Electroluminescence from ZnO Nanowires/p-Si Heterostructure LEDs with MgO Film as Carrier Control Layer. *Journal of The Electrochemical Society*. 2011;159(2):H102-H6.
- Bhat S, V SB, Naik KG. Au catalyst assisted growth of ZnO nanowires by vapour phase transport method on p-Si and fabrication of p-Si/n-ZnO heterojunction diode. AIP Publishing LLC; 2015.
- Choi J-H, Das SN, Moon K-J, Kar JP, Myoung J-M. Fabrication and characterization of p-Si nanowires/ZnO film heterojunction diode. *Solid-State Electronics*. 2010;54(12):1582-5.
- Ku C-S, Huang J-M, Lin C-M, Lee H-Y. Fabrication of epitaxial ZnO films by atomic-layer deposition with interrupted flow. *Thin Solid Films*. 2009;518(5):1373-6.
- Koteeswara Reddy N, Ahsanulhaq Q, Kim JH, Hahn YB. Behavior of n-ZnO nanorods/p-Si heterojunction devices at higher temperatures. *Applied Physics Letters*. 2008;92(4):043127.
- Cao CW, Bao WN, Lin X, Liu XY, Geng Y, Lu HL, et al. N-ZnO Nanowires/p-Si Heterojunction with Amorphous Seed Layer Prepared by Atomic Layer Deposition. *ECS Solid State Letters*. 2013;2(4):Q25-Q8.
- Kale VS, Prabhakar RR, Pramana SS, Rao M, Sow C-H, Jinesh KB, et al. Enhanced electron field emission properties of high aspect ratio silicon nanowire-zinc oxide core-shell arrays. *Physical Chemistry Chemical Physics*. 2012;14(13):4614.

16. Hazra P, Singh SK, Jit S. Impact of surface morphology of Si substrate on performance of Si/ZnO heterojunction devices grown by atomic layer deposition technique. *Journal of Vacuum Science & Technology A: Vacuum, Surfaces, and Films*. 2015;33(1):01A114.
17. Kang H, Park J, Choi T, Jung H, Lee KH, Im S, et al. n-ZnO:N/p-Si nanowire photodiode prepared by atomic layer deposition. *Applied Physics Letters*. 2012;100(4):041117.
18. Ghorbanpour M, Hakimi B, Feizi A. A Comparative Study of Photocatalytic Activity of ZnO/activated Carbon Nanocomposites Prepared by Solid-state and Conventional Precipitation Methods. *Journal of Nanostructures*. 2018;8(3):259-265.
19. Abdallah B, Jazmati AK, Kakhia M. Physical, optical and sensing properties of sprayed zinc doped tin oxide films. *Optik*. 2018;158:1113-22.
20. Jazmati AK, Abdallah B. Optical and Structural Study of ZnO Thin Films Deposited by RF Magnetron Sputtering at Different Thicknesses: a Comparison with Single Crystal. *Materials Research*. 2018;21(3).
21. Shakeri Shamsi M, Ahmadi M, Sabet M. Al Doped ZnO Thin Films; Preparation and Characterization. *Journal of Nanostructures*. 2018;8(4):404-407.
22. Leonardi S. Two-Dimensional Zinc Oxide Nanostructures for Gas Sensor Applications. *Chemosensors*. 2017;5(2):17.
23. Abdallah B, Kakhia M, Abou Shaker S. Deposition of Na<sub>2</sub>WO<sub>4</sub> films by ultrasonic spray pyrolysis: effect of thickness on the crystallographic and sensing properties. *Composite Interfaces*. 2016;23(7):663-74.
24. Alnama K, Abdallah B, Kanaan S. Deposition of ZnS thin film by ultrasonic spray pyrolysis: effect of thickness on the crystallographic and electrical properties. *Composite Interfaces*. 2016;24(5):499-513.
25. Ramdas Bari A, Anil Bari P, Bari RH. Studies on sol-gel dip-coated nanostructured ZnO thin films. *Journal of Nanostructures*. 2019;9(2):326-330.
26. VISHNOI S, KUMAR R, SINGH BP. Effect of substrate on physical properties of pulse laser deposited ZnO thin films. *JOURNAL OF INTENSE PULSED LASERS AND APPLICATIONS IN ADVANCED PHYSICS*. 2014;4(1):35 - 39.
27. Al-Khawaja S, Abdallah B, Abou Shaker S, Kakhia M. Thickness effect on stress, structural, electrical and sensing properties of (0 0 2) preferentially oriented undoped ZnO thin films. *Composite Interfaces*. 2015;22(3):221-31.
28. Gao SY, Li HD, Yuan JJ, Li YA, Yang XX, Liu JW. ZnO nanorods/plates on Si substrate grown by low-temperature hydrothermal reaction. *Applied Surface Science*. 2010;256(9):2781-5.
29. Lujun Y, Maojun Z, Changli L, Li M, Wenzhong S. Facile synthesis of superhydrophobic surface of ZnO nanoflakes: chemical coating and UV-induced wettability conversion. *Nanoscale Research Letters*. 2012;7(1):216.
30. Rusli N, Tanikawa M, Mahmood M, Yasui K, Hashim A. Growth of High-Density Zinc Oxide Nanorods on Porous Silicon by Thermal Evaporation. *Materials*. 2012;5(12):2817-32.
31. Lin H-H, Chen W-H, Hong FCN. Improvement of polycrystalline silicon wafer solar cell efficiency by forming nanoscale pyramids on wafer surface using a self-mask etching technique. *Journal of Vacuum Science & Technology B, Nanotechnology and Microelectronics: Materials, Processing, Measurement, and Phenomena*. 2013;31(3):031401.
32. Pessoa RS, Tezani LL, Maciel HS, Petraconi G, Massi M. Study of SF<sub>6</sub> and SF<sub>6</sub>/O<sub>2</sub> plasmas in a hollow cathode reactive ion etching reactor using Langmuir probe and optical emission spectroscopy techniques. *Plasma Sources Science and Technology*. 2010;19(2):025013.
33. Boulousis G, Constantoudis V, Kokkoris G, Gogolides E. Formation and metrology of dual scale nano-morphology on SF<sub>6</sub> plasma etched silicon surfaces. *Nanotechnology*. 2008;19(25):255301.
34. Choi W, Lee K. Orientation-dependent plasma etch rates of single crystal silicon for dry etcher parts. *International Journal of Materials Research*. 2015;106(11):1123-30.
35. Hazra P, Singh SK, Jit S. Impact of surface morphology of Si substrate on performance of Si/ZnO heterojunction devices grown by atomic layer deposition technique. *Journal of Vacuum Science & Technology A: Vacuum, Surfaces, and Films*. 2015;33(1):01A114.
36. Shin MH, Park MS, Jung SH, Boo JH, Lee NE. Effect of doping elements on ZnO etching characteristics with CH<sub>4</sub>/H<sub>2</sub>/Ar plasma. *Thin Solid Films*. 2007;515(12):4950-4.
37. Park JS, Park HJ, Hahn YB, Yi GC, Yoshikawa A. Dry etching of ZnO films and plasma-induced damage to optical properties. *Journal of Vacuum Science & Technology B: Microelectronics and Nanometer Structures*. 2003;21(2):800.
38. Chang Y-M, Jian S-R, Lee H-Y, Lin C-M, Juang J-Y. Enhanced visible photoluminescence from ultrathin ZnO films grown on Si-nanowires by atomic layer deposition. *Nanotechnology*. 2010;21(38):385705.
39. Wang XN, Wang Y, Mei ZX, Dong J, Zeng ZQ, Yuan HT, et al. Low-temperature interface engineering for high-quality ZnO epitaxy on Si(111) substrate. *Applied Physics Letters*. 2007;90(15):151912.
40. Um H-D, Moiz SA, Park K-T, Jung J-Y, Jee S-W, Ahn CH, et al. Highly selective spectral response with enhanced responsivity of n-ZnO/p-Si radial heterojunction nanowire photodiodes. *Applied Physics Letters*. 2011;98(3):033102.
41. Salimy S, Challali F, Goullet A, Besland MP, Carette M, Gautier N, et al. Electrical Characteristics of TiO<sub>2</sub> Thin Films Deposited on SiO<sub>2</sub>/Si Substrates by Magnetron Sputtering. *ECS Solid State Letters*. 2013;2(3):Q13-Q5.
42. Nayef UM, Muayad MW, Khalaf HA. Effect of ZnO Layers on Porous Silicon Properties. *Int J Electrochem Sci*. 2014;9:2278 - 2284.
43. Inamdar SI, Rajpure KY. High-performance metal-semiconductor-metal UV photodetector based on spray deposited ZnO thin films. *Journal of Alloys and Compounds*. 2014;595:55-9.